Article

Discovery Medicine 2024; 36(191): 2433–2444
https://doi.org/10.24976/Discov.Med.202436191.224

Role of *KIF20A* Depletion in Inhibiting Ovarian Cancer Progression: Insights From *PTEN* and M2 Macrophage Polarization

Xingqiang Wang[1,†], Xiaolong Qian[1,†], Duowen Zhao[2], Ruizhi Xu[2], Zhijie Liu[3,*]

[1]Department of Obstetrics and Gynecology, Gansu University of Chinese Medicine, 730000 Lanzhou, Gansu, China
[2]Department of Obstetrics and Oncology, Gansu Provincial Maternity and Child Health Hospital, 730000 Lanzhou, Gansu, China
[3]Department of the Second Ward of Gynecology, Maternity and Child Health Care Hospital of Gansu Provincial, 730000 Lanzhou, Gansu, China
*Correspondence: l-zj2005@163.com (Zhijie Liu)
[†]These authors contributed equally.
Published: 20 December 2024

Backgrounds: Recent studies have proven the oncogenic role of kinesin family member 20A (*KIF20A*) in several cancers. Tumor-associated macrophages (TAMs) were reported to participate in tumor initiation and metastasis. In this study, we aimed to explore the detailed mechanism underlying *KIF20A* in regulating the progression of ovarian cancer and its involvement with TAMs.
Methods: *KIF20A* and phosphatase and tensin homolog (*PTEN*) levels were assessed using reverse-transcription quantitative polymerase chain reaction (RT-qPCR) and western blot. Cell Counting Kit-8 (CCK-8) assay, 5-Ethynyl-2′-deoxyuridine (EdU) staining assay, colony formation assay, flow cytometry, and western blot were employed to evaluate cell proliferation, apoptosis, and epithelial-mesenchymal transition (EMT). The relationship between *KIF20A* and *PTEN* was validated using a dual-luciferase assay. M2 macrophage polarization was verified by detecting their markers using RT-qPCR. THP-1 cells were co-cultured with ovarian cancer cells to format TAMs.
Results: Ovarian cancer tissues and cells exhibited upregulated *KIF20A* and downregulated *PTEN* levels ($p < 0.05$). Irradiation significantly decreased *KIF20A* levels ($p < 0.05$) and blunted the progression of ovarian cancer by reducing cell proliferation and EMT ($p < 0.05$) and inducing apoptosis ($p < 0.05$). These effects were augmented by *KIF20A* depletion ($p < 0.05$). *KIF20A* depletion also suppressed ovarian cancer cell progression ($p < 0.05$). Our findings illustrated that *KIF20A* negatively regulated PTEN expression in ovarian cancer cells. Moreover, the inhibitory effects of *KIF20A* depletion on ovarian cancer development in irradiated ovarian cancer cells were obviously impeded by *PTEN* knockdown ($p < 0.05$). Additionally, we observed the increased *KIF20A* expression in M2-like TAMs and its ability to induce M2 macrophage polarization ($p < 0.05$).
Conclusion: *KIF20A* was found to induce M2 macrophage polarization in ovarian cancer, and *KIF20A* depletion regulated *PTEN* to increase radiosensitivity and inhibit ovarian cancer development.

Keywords: *KIF20A*; ovarian cancer; TAMs; *PTEN*; macrophage polarization

Introduction

Ovarian cancer is a prevalently fatal gynecologic malignancy, with approximately 22,440 new cases annually and 14,080 deaths per year [1]. The mortality rate of ovarian cancer is particularly high due to the frequency of late-stage diagnoses, where metastasis has spread beyond pelvic organs and ovaries to the abdominal and peritoneum organs, including the liver, omentum, stomach, diaphragm, and intestines [2]. Currently, the standard therapeutic management methods for ovarian cancer include adjuvant radiotherapy, adjuvant chemotherapy, and cytoreductive surgery [3,4]. Despite the significant advancement of new therapeutic reagents, the death rate of ovarian cancer remains the highest among all gynecological cancers [5]. In radiotherapy treatment, the development of treatment resistance commonly influences the efficacy. Despite the accumulating knowledge about ovarian cancer, the mechanisms related to radiosensitivity are not fully understood.

Collective evidence has revealed the close correlation between the tumor microenvironment (TME) and tumor initiation, development, metastasis, and treatment outcomes across different types of cancers [6–8]. The intricate interactions between tumor cells and other cells within the TME play an essential role in cancer progression [9]. Various cytokines and cells have been consistently observed in the TME, including cancer cells, non-cellular components, cancer-associated fibroblasts, and tumor-associated macrophages (TAMs) [10,11]. Among them, TAMs secrete diverse mediators such as chemokines or cytokines. These mediators stimulate angiogenesis, repress anti-cancer immune responses, and boost tumor cell intravasation, proliferation, and dissemination for metastasis [12]. Given the

crucial role of TAMs in tumor development, treating them has emerged as a novel therapeutic approach for cancer treatment [13,14]. TAMs are typically categorized into two main types based on different stimuli-induced polarization programs: alternative M2 macrophages and classically activated M1 macrophages. Interestingly, M2 macrophages contribute to cancer progression by disrupting inflammatory circuits and adaptive immunity, whereas classical M1 macrophages exhibit pro-immunity, pro-inflammatory, and anti-cancer functions [15–17]. Although the tumor-promoting functions of M2-like TAMs have been well illustrated, the possible mechanisms of M2-like TAMs polarization remain largely unclear.

Several members of the kinesin family (*KIF*) possess adenosine triphosphate (ATP) activity and play essential roles in various physiological functions such as substance transport, chromosome partitioning, and intracellular spindle formation. Kinesin family member 20A (*KIF20A*) mainly accumulates in the central region of the mitotic cell spindle and contributes to cell mitosis by regulating midbody separation, microtubule bundle formation, and cytokinesis [18,19]. *KIF20A*-related pathways include responses to cytosolic Ca^{2+} acceleration, cell mitosis, and the cell cycle [20]. Previous research has verified the increased expression of *KIF20A* in various cancers [21–23]. For instance, the *KIF20A* has been shown to contribute to the progression of colorectal cancer by regulating the Warburg effects [24]. However, the specific regulation of *KIF20A* in ovarian cancer and its underlying mechanisms have yet to be studied.

In the present study, we attempted to probe the functional role of *KIF20A* in ovarian cancer. After proving the increased expression of *KIF20A* in ovarian cancer, we then excavated how *KIF20A* affected radiosensitivity, macrophage polarization, and ovarian cancer development to investigate its potential underlying mechanisms.

Materials and Methods

Patients and Specimens

Fifty paired samples of ovarian cancer and adjacent normal ovarian tissues (at least 5 cm away from the tumor tissues) were obtained from 50 ovarian cancer patients during curative resection at Gansu University of Chinese Medicine. Inclusion criteria included: no adjuvant preoperative radiotherapy or chemotherapy started before admission; complete medical records. Exclusion criteria included: a history of other malignancies and recurrent ovarian cancer. All patients signed the written informed contents, and the project was conducted based on the Declaration of Helsinki statement. This study protocol was approved by the Medical Ethics Committee of Gansu University of Chinese Medicine (2021-48KYSL).

Cell Culture, Transfection, and Irradiation

IOSE80 (FY-H37149; FUYUBIO, Shanghai, China), SKOV3 (FY-G26696; FUYUBIO, Shanghai, China), A2780 (FY-22FN0790; FUYUBIO, Shanghai, China), and THP-1 cells (TIB-202™; ATCC, Manassas, VA, USA) were cultured in Roswell Park Memorial Institute (RPMI)-1640 medium (31800022; Gibco, GrandIsland, NY, USA) and supplemented with 10% fetal bovine serum (FBS) (10099-141; Gibco, GrandIsland, NY, USA). Cultures were maintained at a constant temperature of 37 °C in a humidified atmosphere with 95% O_2 and 5% CO_2. All cell lines had been authenticated using Short Tandem Repeats (STR) profiling, and mycoplasma testing confirmed the absence of contamination.

The oligonucleotides included si*RNA* against *KIF20A* (si-*KIF20A*; 5′-CUGUGAAGGAGAUGGUAAATT-3′; sc-91657A; Santa Cruz Biotechnology, Santa Cruz, CA, USA) and si*RNA* against phosphatase and tensin homolog (si-*PTEN*; 5′-GGTCAAGTGAAGACGACAA-3′; siB101025113730-1-5; RiboBio, Guangzhou, China), and the negative control (si-NC; 5′-CUUACGCUGAGUACUUCGATT-3′; siN0000002-1-5; RiboBio, Guangzhou, China). The *KIF20A*-overexpression plasmid (*KIF20A*; CMV-*KIF20A*-EGFP-SV40-Neomycin, Genechem, Shanghai, China) was obtained by amplifying the full length of *KIF20A* and inserting it into GV230 (Genechem, Shanghai, China), with an empty GV230 plasmid (pcDNA) as the scramble control. Lipofectamine 3000 (Invitrogen, Carlsbad, CA, USA) was used to complete cell transfection.

Irradiation was conducted according to previous research [25]. An exposure instrument, Cs-137 irradiator (HWMD-2000, Siemens, Munich, Germany) was employed to carry out X-ray irradiation with the single dose of 4 Gy on SKOV3 and A2780 cells. The irradiated cells were collected every 6 hours for further analysis within 24 hours.

Reverse-Transcription Quantitative Polymerase Chain Reaction (RT-qPCR) Analysis

Total RNA extraction was conducted with Trizol Reagent (15596018CN; Invitrogen, Carlsbad, CA, USA) according to the manufacturer's instructions. Reverse transcription to synthesize cDNA from total *RNA* was executed via the Primescript™ RT reagent Kit (RR014A; Takara, Tokyo, Japan). RT-qPCR analysis was preceded on the BIO-RAD CFX96 Real-time PCR machine (Bio-Rad, Hercules, CA, USA) with the usage of the SYBR-Green PCR Master Mix (Vazyme.Q111-02; Vazyme, Nanjing, China). The relative expression levels were normalized by glyceraldehyde-3-phosphate dehydrogenase (*GAPDH*) and computed by the $2^{-\Delta\Delta Ct}$ method. The PCR program was as follows: denaturation at 95 °C for 10 min, denaturation at 95 °C for 30 s (40 cycles), annealing at 60 °C for 30 s, and extension at 72 °C for 1 min. The sequences of

all primers used were: *KIF20A*, F 5′-CAAGGGATCCT TTCTCCGCC-3′, R 5′-GAACCTGCTGCTTGTCCTC T-3′; *PTEN*, F 5′-TCCCAGACATGACAGCCATC-3′ , R 5′-TGCTTTGAATCCAAAAACCTTACT-3′; tumor necrosis factor-alpha (*TNF-α*), F 5′-GCCTCTTCTCATT CCTGCTTG-3′, R 5′-GGCCATTTGGGAACTTCTCA-3 ′; C-X-C motif Chemokine Ligand 10 (*CXCL10*), F 5′-C AAATCTGCTTTTTAAAGAATGCTC-3′, R 5′-AAGA ATTTGGGCCCCTTG-3′; human leukocyte antigen-DR (*HLA-DR*), F 5′-TCTGGCGGCTTGAAGAATTTG-3′, R 5′-GGTGATCGGAGTATAGTTGGAGC-3′; cluster of differentiation 163 (*CD163*), F 5′-TTGTCAACTTGAG TCCCTTCAC-3′, R 5′-TCCCGCTACACTTGTTTTCA C-3′; cluster of differentiation 206 (*CD206*), F 5′-GGG TTGCTATCACTCTCTATGC-3′, R 5′-TTTCTTGTCT GTTGCCGTAGTT-3′; arginase-1 (*ARG1*), F 5′-TGGA CAGACTAGGAATTGGCA-3′, R 5′-CCAGTCCGTC AACATCAAAACT-3′; transforming growth factor-beta (*TGF-β*), F 5′-AAGGACCTCGGCTGGAAGTGC-3′, R 5′-CCGGGTTATGCTGGTTGTA-3′; interleukin-10 (*IL-10*), F 5′-GCCAAGCCTTGTCTGAGATGATCC-3′, R 5′-TTCACATGCGCCTTGATGTCTGG-3′; *GAPDH*, F 5′-GCACCACCAACTGCTTAGCA-3′, R 5′-GTCTTCTGGGTGGCAGTGATG-3′.

Western Blot

Following total protein collection, the proteins were separated on 10% sodium dodecyl sulfate-polyacrylamide gel electrophoresis (SDS-PAGE). Subsequently, the proteins were transferred onto polyvinylidene fluoride (PVDF) membranes and blocked by 5% non-fat milk for 1.5 hours. The membranes were then incubated with the primary antibodies at 4 °C overnight, followed by incubation with horseradish peroxidase (HRP)-conjugated secondary antibodies (ab6721 and ab6789; 1:2000; Abcam, Cambridge, UK) at room temperature for 1.5 hours. The primary antibodies were anti-vimentin (ab92547; 1:2000; Abcam, Cambridge, UK), anti- KIF20A (sc-374508; 1:1000; Santa Cruz Biotechnology, Santa Cruz, CA, USA), anti-E-cadherin (#3195; 1:1000; Cell Signaling Technology, Danvers, MA, USA), anti-PTEN (9188; 1:1000; Cell Signaling Technology, Danvers, MA, USA), anti-N-cadherin (ab76011; 1:2000; Abcam, Cambridge, UK), and anti-GAPDH (ab181602; 1:1000; Abcam, Cambridge, UK). Protein visualization was performed using enhanced chemiluminescence (WBULP-100ML; Millipore, Bradford, MA, USA). The signals of the protein complexes were semi-quantified by ImageJ software (Version 1.52b, NIH, Bethesda, MD, USA).

Cell Proliferation

The cell viability of SKOV3 and A2780 cells was assessed using the Cell Counting Kit-8 (CCK-8) kit (C0038; Beyotime, Shanghai, China). Initially, 4000 SKOV3 and A2780 cells were plated on the 96-well plate. After irradiation under 4 Gy and transfection with the oligonucleotides, the treated cells were co-cultured with the CCK-8 solution. After 2 hours, cell viability was evaluated by assessing the absorbance at 450 nm through a microplate reader (Multiskan MK3; Thermo Labsystems, Waltham, MA, USA). For the 5-Ethynyl-2′-deoxyuridine (EdU) assay, co-culture of EdU regent (C10338; RiboBio, Guangzhou, China) and the treated SKOV3 and A2780 cells was also carried out for 2 hours. Subsequently, the cells were stained with 4′,6-diamidino-2-phenylindole (DAPI) for 15 minutes to label the nuclei. The EdU-positive cells were observed and quantified using a fluorescent microscope (ZEISS Axioscope 5, Carl Zeiss AG, Heidenheim, Germany).

Colony Formation Assay

SKOV3 and A2780 cells (500 cells) were cultured in 6-well plates for 14 days. The colonies were then observed, fixed, and dyed with crystal violet (C0121; Beyotime, Shanghai, China). Finally, the number of colonies was counted (clones with over 50 cells) using a fluorescent microscope (ZEISS Axioscope 5, Carl Zeiss AG, Heidenheim, Germany).

Flow Cytometry

The apoptotic cells were determined using the Annexin V-fluorescein isothiocyanate (FITC) apoptosis detection kit (C1062L; Beyotime, Shanghai, China) according to the manufacturer's instructions. The treated SKOV3 and A2780 cells were suspended in a cell suspension and incubated with Annexin V-FITC and propidium iodide (PI). After incubation for 15 min without light, the apoptotic cells were analyzed via flow cytometry (FACSymphony™A3; BD, Franklin Lakes, NJ, USA). The rate of apoptosis was presented as the percentage of early and late apoptotic cells relative to the total number of cells. Early apoptotic cells were identified as (AnnexinV-FITC)+/PI–, while late apoptotic cells were identified as (AnnexinV-FITC)+/PI+.

Determination of Promoter Activity Using a Dual-Luciferase Reporter Assay

To generate the pGL3-PTEN construct, the promoter region of PTEN was amplified and inserted into the pGL3-Basic vector. Subsequently, the KIF20A-overexpressing vector, pGL3-PTEN, and renilla luciferase vector (pRL-TK; Promega, Madison, WI, USA) were transfected into HEK293T cells to detect the influence of luciferase activity with the usage of Dual-Luciferase Reporter Assay System (Promega.e1960, Promega, Madison, WI, USA).

Macrophage Generation and Polarization

THP-1 cells were treated with phorbol-12-myristate-13 acetate (PMA; 100 ng/mL; P1585; Sigma-Aldrich, St. Louis, MO, USA) for 24 hours to induce differentiation into M0 macrophages. Subsequently, M0 macrophages were further polarized into M1 macrophages by treat-

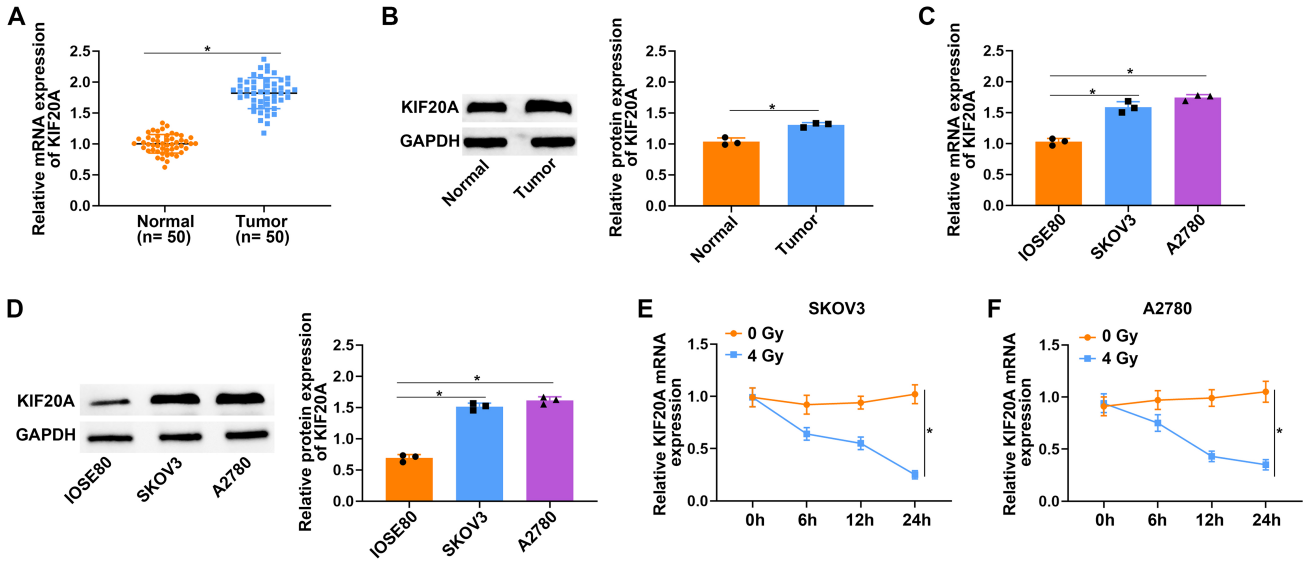

Fig. 1. *KIF20A* was reduced by radiation in ovarian cancer cells. (A) Determination of *KIF20A* mRNA expression in ovarian cancer tissues (n = 50) and normal ovarian tissues (n = 50) using RT-qPCR. (B) KIF20A protein expression in ovarian cancer tissues and normal ovarian tissues was detected by western blot (n = 3). (C,D) Assessment of KIF20A mRNA and protein expression in IOSE80 cells and ovarian cancer cells using RT-qPCR and western blot, respectively (n = 3). (E,F) Measurement of *KIF20A mRNA* levels in SKOV3 and A2780 cells after 4 Gy radiation using RT-qPCR (n = 3). *$p < 0.05$. *KIF20A*, kinesin family member 20A; RT-qPCR, reverse-transcription quantitative polymerase chain reaction; *GAPDH*, glyceraldehyde-3-phosphate dehydrogenase.

ment with 50 ng/mL of lipopolysaccharide (LPS; L8274; Sigma-Aldrich, St. Louis, MO, USA) and 20 ng/mL of interferon-gamma (IFN-γ; SRP3058; Sigma-Aldrich, St. Louis, MO, USA), or into M2 macrophages with 25 ng/mL of interleukin-4 (IL-4; SRP3093; Sigma-Aldrich, St. Louis, MO, USA) and 20 ng/mL of interleukin-13 (IL-13; SRP3274; Sigma-Aldrich, St. Louis, MO, USA) for 48 hours. Following polarization, TAMs were formatted by co-culturing M0 macrophages with ovarian cancer cells (SKOV3 and A2780 cells). After 48 hours, TAMs were acquired by collecting the co-cultured macrophages.

Statistics Analysis

All results were presented as means ± standard deviation from three independent replicates. Data were analyzed using GraphPad Prism 7.0 (GraphPad Software Inc., San Diego, CA, USA). A paired *t*-test was used to compare tumor tissues with adjacent tissues. The difference in measurement data was compared using Student's *t*-test between groups or one-way analysis of variance (ANOVA) with post hoc Tukey's test for multiple groups. A statistically significant difference was obtained when $p < 0.05$.

Results

KIF20A was Reduced by Radiation in Ovarian Cancer Cells

To identify the role of *KIF20A* in ovarian cancer, we initially analyzed *KIF20A* expression in ovarian cancer tissues. The elevated mRNA and protein expression of KIF20A was demonstrated in ovarian cancer tissues (n = 50) collected from ovarian cancer patients in comparison to the adjacent normal ovarian tissues (n = 50) ($p < 0.05$) (Fig. 1A,B). Furthermore, we also examined the *mRNA* and protein levels of KIF20A in ovarian cancer cell lines (SKOV3 and A2780 cells) and human ovarian epithelial cell lines (IOSE80 cells). The *mRNA* and protein expression of KIF20A were significantly increased in SKOV3 and A2780 cells ($p < 0.05$) (Fig. 1C,D). Additionally, the data in Fig. 1E,F displayed that 4 Gy radiation caused a remarkable reduction of *KIF20A* in SKOV3 and A2780 cells ($p < 0.05$).

KIF20A Depletion Enhanced Radiation-Caused Suppressive Effects on Cell Proliferation and Epithelial-Mesenchymal Transition (EMT), as well as Enhancement Effect on Apoptosis in Ovarian Cancer Cells

The western blot analysis revealed a significant reduction in KIF20A protein expression after transfection of si-*KIF20A* in SKOV3 and A2780 cells ($p < 0.05$) (Fig. 2A). Additionally, the CCK-8 assay demonstrated a notable decrease in cell viability in SKOV3 and A2780 cells after exposure to 4 Gy radiation ($p < 0.05$), which was further exacerbated after downregulating *KIF20A* ($p < 0.05$) (Fig. 2B). Similar results were found in both the EdU and colony formation assays ($p < 0.05$). Specifically, the EdU-positive cells and colonies of SKOV3 and A2780 cells significantly decreased followed exposure to 4 Gy radiation ($p < 0.05$), and knockdown of *KIF20A* aggravated its ef-

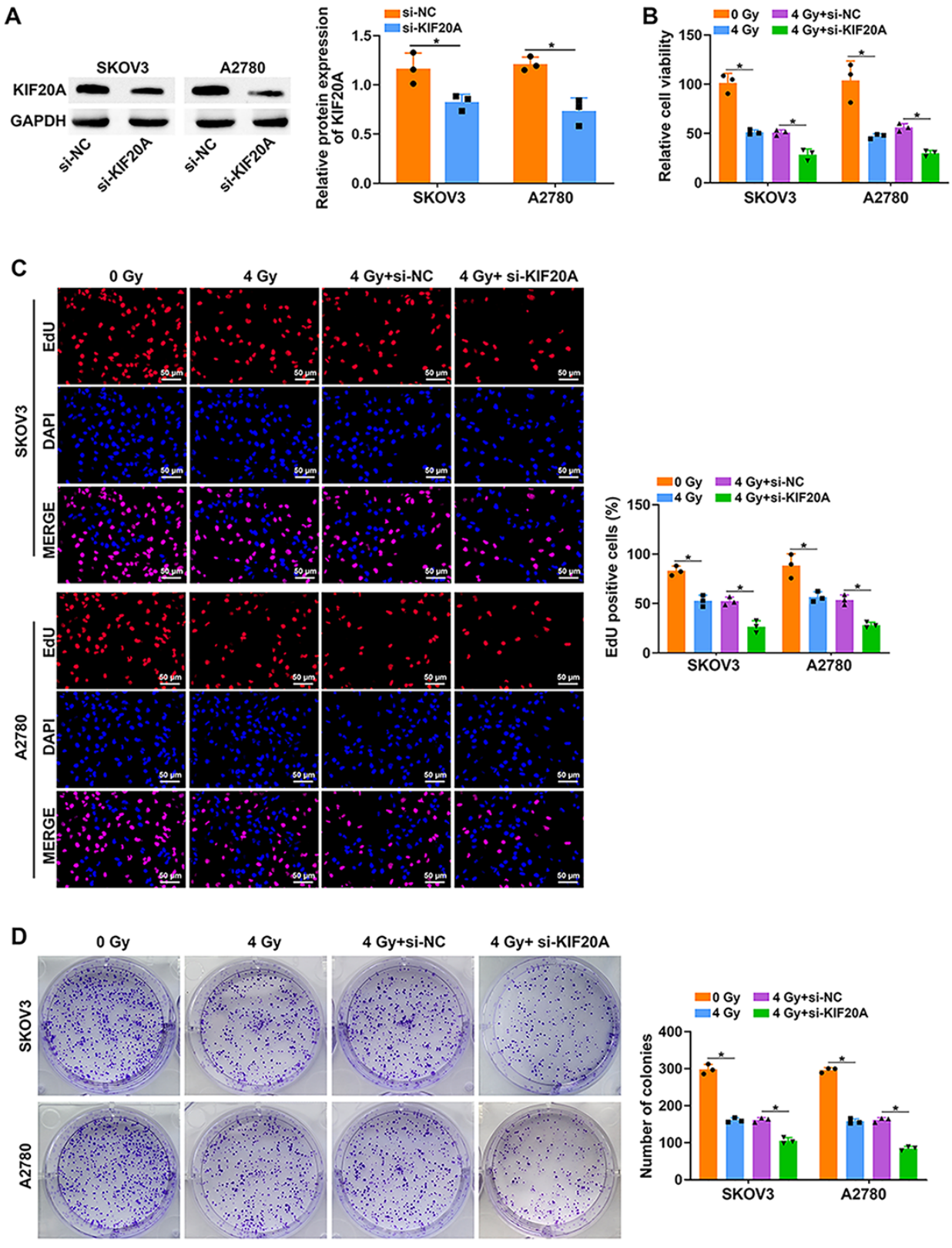

Fig. 2. *KIF20A* depletion aggravated radiation-caused suppressive effects on cell proliferation and EMT in ovarian cancer cells. (A) The knockdown efficiency of si-*KIF20A* was tested using a western blot (n = 3). (B–D) SKOV3 and A2780 cells were treated with 0 Gy radiation, 4 Gy radiation, 4 Gy+si-NC, or 4 Gy+si-*KIF20A*. (B) CCK-8 assay for detecting cell viability (n = 3). (C) EdU staining assay for assessing the EdU-positive cells (n = 3). Scale bar: 50 μm. (D) Colony formation assay for determining the number of colonies (n = 3). *$p < 0.05$. EMT, epithelial-mesenchymal transition; CCK-8, Cell Counting Kit-8; EdU, 5-Ethynyl-2′-deoxyuridine.

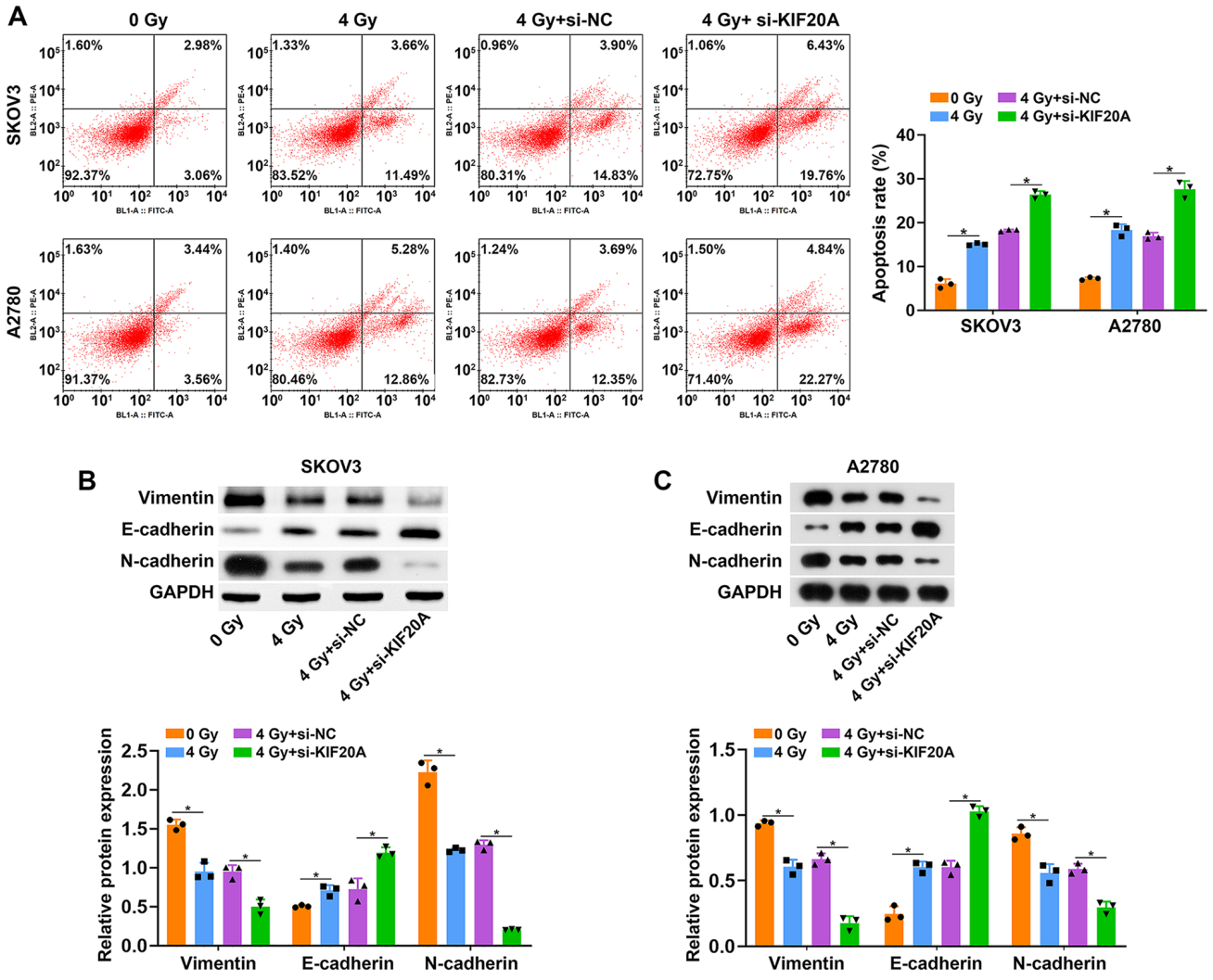

Fig. 3. *KIF20A* depletion enhanced radiation-induced apoptosis in ovarian cancer cells. (A) Flow cytometry for evaluating the apoptotic rate (n = 3). (B,C) Western blot for measuring the protein expression of EMT-associated proteins (Vimentin, N-cadherin, and E-cadherin) (n = 3). *$p < 0.05$.

fects on cell proliferation ($p < 0.05$) (Fig. 2C,D). Moreover, 4 Gy radiation triggered cell apoptosis was further facilitated by *KIF20A* depletion in SKOV3 and A2780 cells ($p < 0.05$) (Fig. 3A). Furthermore, our results demonstrated that *KIF20A* depletion also could augment the repressive impact of 4 Gy radiation on EMT ($p < 0.05$), as evidenced by lower vimentin and N-cadherin levels, and increased E-cadherin levels in SKOV3 and A2780 cells treated with 4 Gy+si-*KIF20A* compared to cells treated with 4 Gy radiation alone ($p < 0.05$) (Fig. 3B,C). These findings revealed that *KIF20A* depletion could elevate radiosensitivity in ovarian cancer cells.

PTEN was Downregulated in Ovarian Cancer, and KIF20A Negatively Regulated PTEN Expression in Ovarian Cancer Cells

PTEN mRNA and protein expression were significantly lower in ovarian cancer tissues relative to normal ovarian tissues ($p < 0.05$) (Fig. 4A,B). In SKOV3 and A2780 cells, *PTEN* mRNA and protein levels were markedly reduced compared to IOSE80 cells ($p < 0.05$) (Fig. 4C,D). Moreover, we observed an elevated PTEN protein expression in *KIF20A*-silenced SKOV3 and A2780 cells ($p < 0.05$) (Fig. 4E). Radiation (4 Gy) significantly increased *PTEN* mRNA expression in SKOV3 and A2780 cells ($p < 0.05$) (Fig. 4F). Additionally, dual-luciferase assay revealed that *KIF20A* suppressed the promoter activity of *PTEN* in HEK293T cells ($p < 0.05$) (Fig. 4G).

PTEN Knockdown Could Partially Reverse the Promotion Effect of KIF20A Depletion on Radiosensitivity in Ovarian Cancer Cells

To investigate the regulatory mechanism between *KIF20A* and *PTEN* in ovarian cancer progression, SKOV3 and A2780 cells were treated with 4 Gy+si-NC, 4 Gy+si-*KIF20A*, 4 Gy+si-*KIF20A*+si-NC, or 4 Gy+si-*KIF20A*+si-

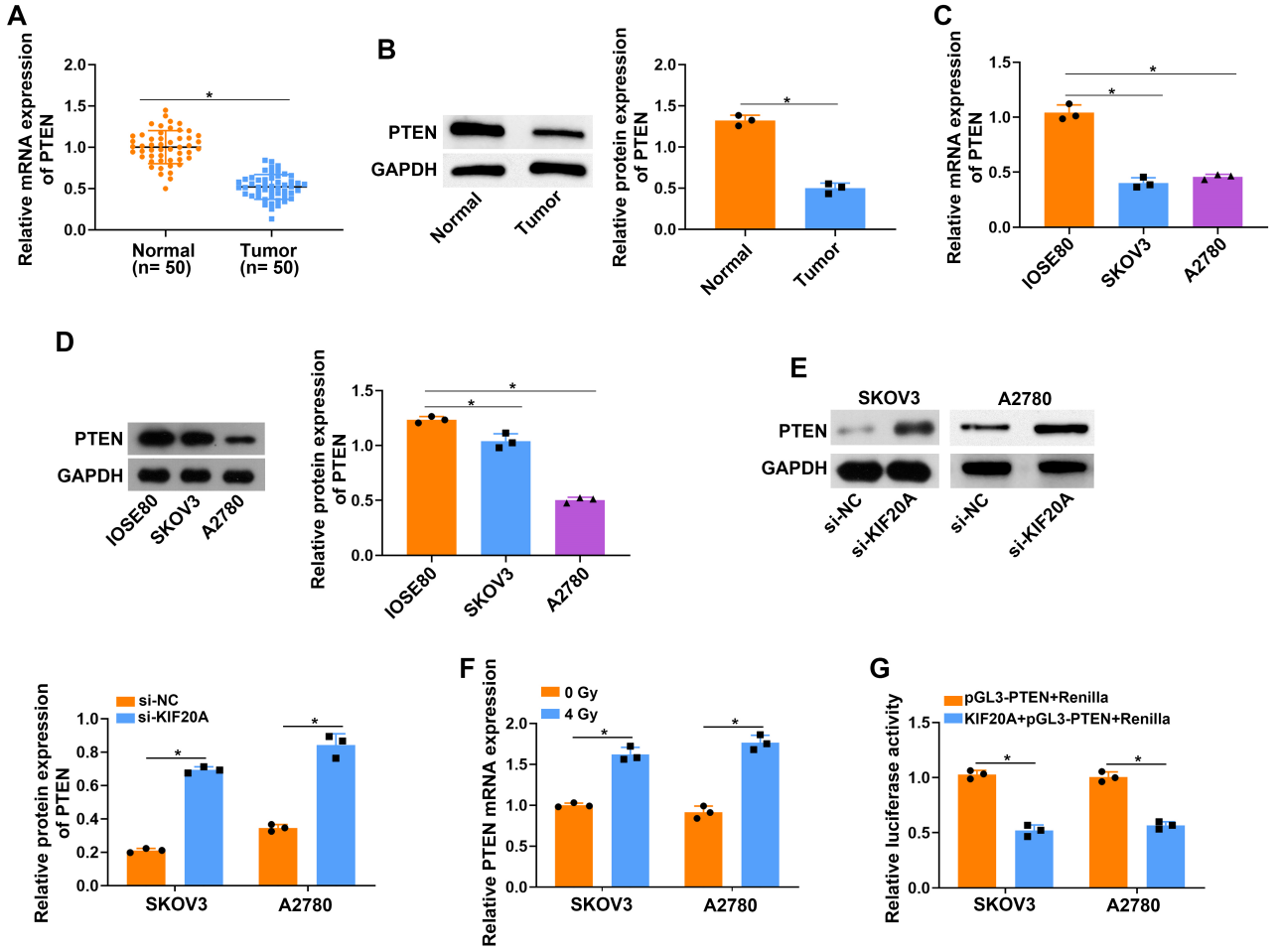

Fig. 4. *PTEN* was downregulated in ovarian cancer, and *KIF20A* negatively regulated *PTEN* expression in ovarian cancer cells. (A) Detection of *PTEN* mRNA in ovarian cancer tissues (n = 50) and normal ovarian tissues (n = 50) using RT-qPCR. (B) PTEN protein expression in ovarian cancer tissues and normal ovarian tissues was measured by western blot (n = 3). (C,D) Measurement of PTEN mRNA and protein expression in IOSE80 cells and ovarian cancer cells using RT-qPCR and western blot, respectively (n = 3). (E) Assessment of PTEN protein expression after *KIF20A* knockdown in ovarian cancer cells was performed via western blot (n = 3). (F) Detection of *PTEN* mRNA level in SKOV3 and A2780 cells after 4 Gy radiation using RT-qPCR (n = 3). (G) The *PTEN* promoter luciferase activity was assessed using a dual-luciferase assay (n = 3). *$p < 0.05$. *PTEN*, phosphatase and tensin homolog.

PTEN. The knockdown efficacy of si-*PTEN* was demonstrated in SKOV3 and A2780 cells ($p < 0.05$) (Fig. 5A). Moreover, the increase in PTEN expression resulting from *KIF20A* depletion was blocked by transfection of si-*PTEN* in 4 Gy irradiated SKOV3 and A2780 cells ($p < 0.05$) (Fig. 5B). The results from Fig. 5C–E demonstrated that the decrease in cell proliferation caused by PTEN upregulation in SKOV3 and A2780 cells exposed to 4 Gy radiation was counteracted by *PTEN* knockdown ($p < 0.05$). *KIF20A* depletion resulted in the enhancement of apoptosis in SKOV3 and A2780 cells exposed to 4 Gy radiation ($p < 0.05$), which was restored by *PTEN* knockdown ($p < 0.05$) (Fig. 6A). Moreover, *PTEN* downregulation attenuated the inhibitory effect of *KIF20A* depletion on EMT in SKOV3 and A2780 cells exposed to 4 Gy radiation ($p < 0.05$) (Fig. 6B,C).

KIF20A was Highly Expressed in M2-Like TAMs and Induced M2 Macrophage Polarization

To validate the effect of *KIF20A* on macrophage polarization, an *in vitro* TAM model was generated according to previous reports [26]. In brief, human THP-1 monocytes were stimulated with PMA for 24 h to differentiate into M0 macrophages, which were then co-cultured with ovarian cancer cells (SKOV3 and A2780 cells) for 48 hours to generate TAMs. TAM_{SKOV3} and TAM_{A2780} exhibited increased expression of M2 markers (*ARG1*, *TGF-*β, *IL-10*, *CD206*, and *CD163*) and decreased expression of M1 markers (*TNF-*α, *CXCL10*, and *HLA-DR*) ($p < 0.05$) (Fig. 7A). Moreover, our data indicated the upregulation of *KIF20A* in TAM_{SKOV3} and TAM_{A2780} ($p < 0.05$), as well as M2 macrophages ($p < 0.05$) (Fig. 7B). To evaluate the role of *KIF20A* in macrophage polarization, M0

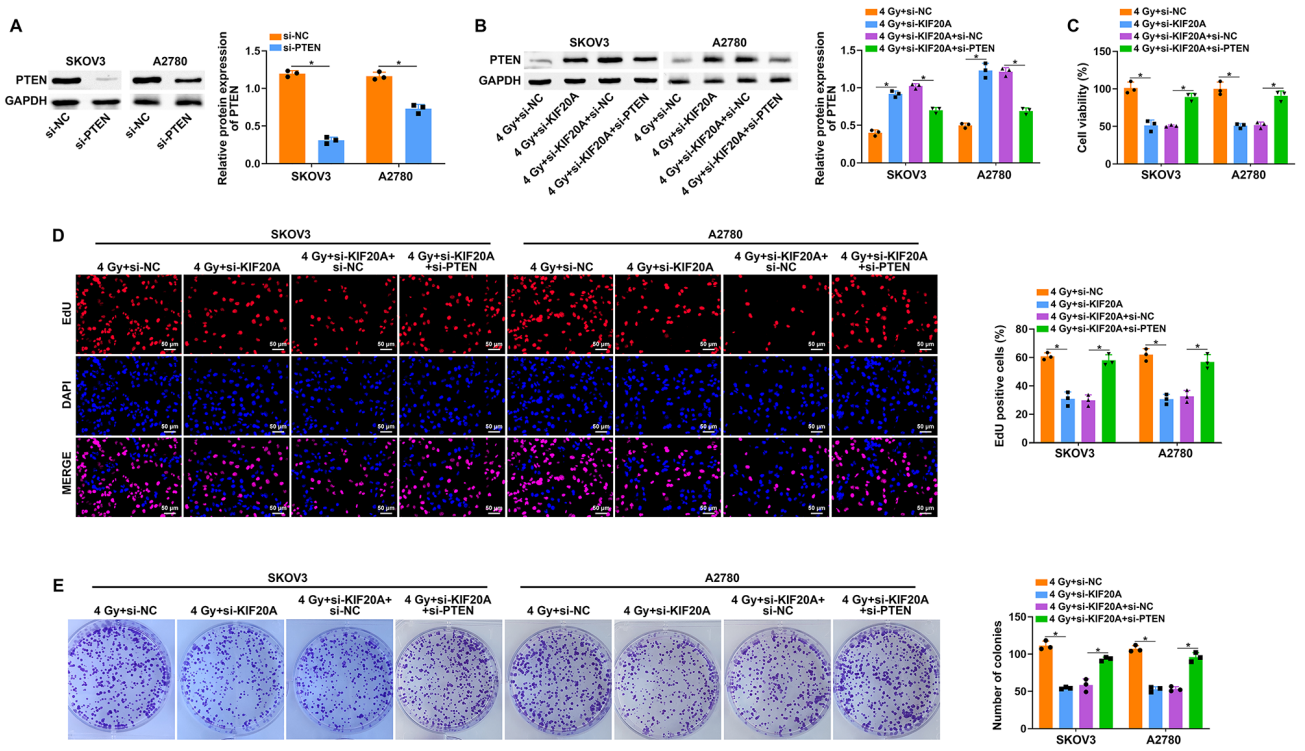

Fig. 5. *PTEN* knockdown could partially reverse the promotional effect of *KIF20A* depletion on radiosensitivity in ovarian cancer cells. (A) The knockdown efficiency of si-*PTEN* was tested using western blot (n = 3). (B) After SKOV3 and A2780 cells were treated with 4 Gy+si-NC, 4 Gy+si-*KIF20A*, 4 Gy+si-*KIF20A*+si-NC, or 4 Gy+si-*KIF20A*+si-*PTEN*, PTEN protein expression was detected using western blot, and (C–E) cell proliferation was evaluated using CCK-8, EdU (Scale bar: 50 μm), and colony formation assays (n = 3). **p* < 0.05.

macrophages were transfected with *KIF20A* overexpression plasmids. The results revealed significantly higher levels of *CD206* and *CD163* in *KIF20A*-overexpressed M0 macrophages compared to untreated M0 macrophages ($p < 0.05$) (Fig. 7C). These findings illustrated the promotional role of *KIF20A* in M2 macrophage polarization.

Discussion

In this study, the results illustrated that *KIF20A* depletion promoted radiosensitivity and blunted the progression of ovarian cancer. *KIF20A* depletion could upregulate *PTEN* expression, a known tumor suppressor. Furthermore, we observed that the effects of *KIF20A* on radiosensitivity and progression of ovarian cancer were mediated by *PTEN*. Moreover, *KIF20A* induced M2 macrophage polarization. Collectively, our findings suggested that *KIF20A* depletion impeded the development of ovarian cancer by regulating *PTEN* expression and regulating M2 macrophage polarization.

Numerous studies have recently displayed a remarkable elevation of *KIF20A* in various tumors, including gastric, breast, liver, and lung cancers, thereby demonstrating the essential role of *KIF20A* in cancer progression [20,24,27,28]. In line with these results, our data also showed a pronounced increase in *KIF20A* expression in ovarian cancer tissues and cells. Moreover, a report indicated that *KIF20A* might dramatically boost ovarian clear-cell carcinoma cell proliferation [29]. In colorectal cancer, *KIF20A* modulated the JAK/STAT3 signaling pathway to affect cell growth [30]. Additionally, its significance in tumorigenesis, progression, and metastasis in prostate cancer has been confirmed [31]. It was reported that *KIF20A* was associated with the activity of bladder cancer cells, and even affected survival level [32]. In this study, the data revealed a significant decrease in *KIF20A* expression in ovarian cancer cells, and *KIF20A* was decreased in irradiated ovarian cancer cells, suggesting that *KIF20A* might be a regulator involved in radiosensitivity in ovarian cancer. To identify the relationship between *KIF20A* and radiosensitivity, as well as the functions of *KIF20A* on ovarian cancer progression, *KIF20A* was knocked down in ovarian cancer cells. Our results showed that irradiation markedly suppressed the development of ovarian cancer. Furthermore, *KIF20A* depletion could suppress cell proliferation and EMT, while inducing apoptosis in irradiated ovarian cancer cells, demonstrating that *KIF20A* depletion significantly increased radiosensitivity in ovarian cancer and further retarded its development.

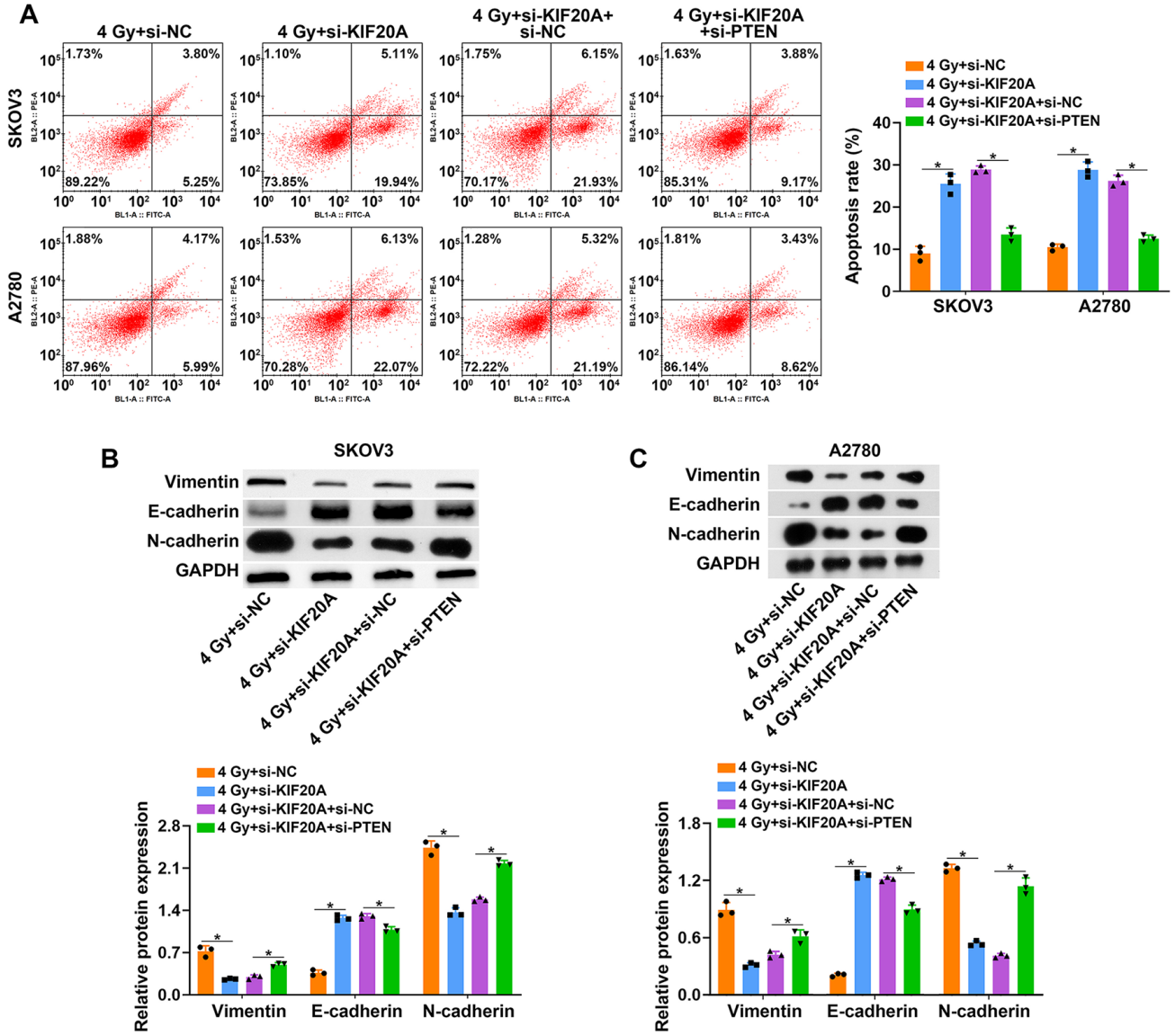

Fig. 6. *PTEN* knockdown could rescue the effects of *KIF20A* depletion on cell apoptosis and EMT in ovarian cancer cells. SKOV3 and A2780 cells were treated with 4 Gy+si-NC, 4 Gy+si-*KIF20A*, 4 Gy+si-*KIF20A*+si-NC, or 4 Gy+si-*KIF20A*+si-*PTEN*. (A) Cell apoptosis was assessed using flow cytometry (n = 3). (B,C) Western blot was used to determine EMT-related protein expression (n = 3). *$p < 0.05$.

PTEN, as a well-known tumor suppressor gene, was demonstrated as a key regulator in tumor apoptosis, differentiation, and proliferation [33–35]. *PTEN* exerts its tumor-suppressive effects by negatively modulating the phosphatidylinositol 3-kinase (PI3K)/protein kinase B (AKT) pathway, thereby influencing processes such as EMT, apoptosis, and DNA damage during tumor development [36–38]. Multiple studies indicated that downregulated *PTEN* levels were observed in various types of cancers, including ovarian cancer [39,40]. Consistently, our data exhibited a significant reduction in *PTEN* levels in ovarian cancer tissues and cells. Moreover, the negative correlation between *KIF20A* and *PTEN* was obtained, and *KIF20A* depletion remarkably elevated *PTEN* expression. Besides, the effects of *KIF20A* depletion on radiosensitivity and cancer progression in ovarian cancer cells were mitigated by *PTEN* knockdown, suggesting the vital role of *KIF20A*/*PTEN* axis in ovarian cancer radiosensitivity and development.

M2 polarization of TAMs is a complex pathological process involving multiple steps and factors in the TME. Previous research has indicated that colorectal cancer cells secrete IL-4, which can promote M2 polarization of TAMs [41]. Furthermore, factors like exosomes [42] and granulocyte-macrophage colony-stimulating factor (GM-CSF) [43] from tumor cells, and fatty acids were verified to participate in the induction of macrophage M2 polarization. Thus, multiple factors from TME or tumor cells were able to impact the M2 polarization of macrophages in cancer

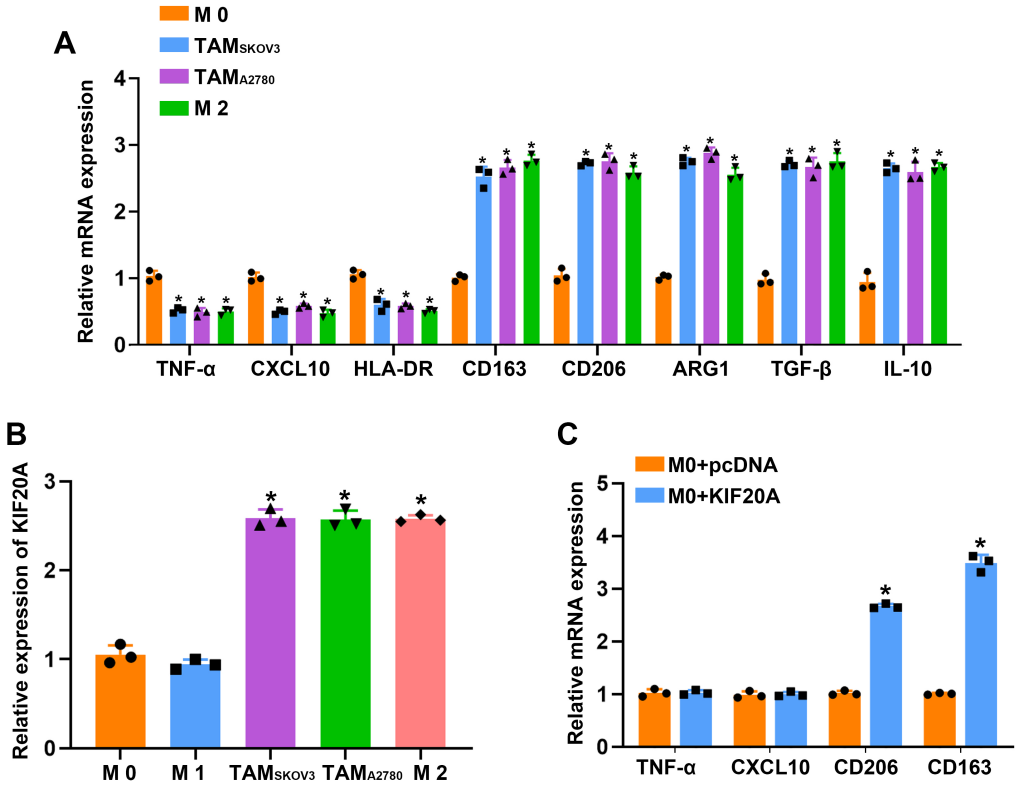

Fig. 7. *KIF20A* was highly expressed in M2-like tumor-associated macrophages (TAMs) and induced M2 macrophage polarization. (A) RT-qPCR analysis of relative levels of both M1 markers (*TNF-α*, *CXCL10*, and *HLA-DR*) and M2 markers (*ARG1*, *TGF-β*, *IL-10*, *CD206*, and *CD163*) in M0 and M2 macrophages, as well as TAMs co-cultured with KOV3 and A2780 cells for 48 hours (n = 3). *$p < 0.05$ compared with M0. (B) RT-qPCR analysis of *KIF20A* expression levels in M0 and M2 macrophages, as well as TAMs co-cultured with KOV3 and A2780 cells for 48 hours (n = 3). *$p < 0.05$ compared with M0. (C) The levels of M1 markers (*TNF-α* and *CXCL10*) and M2 markers (*CD163* and CD206) in *KIF20A*-overexpressed M0 macrophages using RT-qPCR (n = 3). *$p < 0.05$ compared with M0+pcDNA. TAMs, tumor-associated macrophages; *TNF-α*, tumor necrosis factor-alpha; *CXCL10*, C-X-C motif Chemokine Ligand 10; *HLA-DR*, human leukocyte antigen-DR; *CD163*, cluster of differentiation 163; *CD206*, cluster of differentiation 206; *ARG1*, arginase-1; *TGF-β*, transforming growth factor-beta; *IL-10*, interleukin-10.

progression. M2 macrophages are known to accelerate tumor immune escape and suppress inflammatory responses, thereby demonstrating their tumor-promoting function [44]. Recent research reported that wingless-type MMTV integration site family member 5a (*WNT5a*), a highly expressed gene in colorectal cancer, caused M2 polarization of TAMs, thereby boosting the progression of colorectal cancer [45]. In the present study, overexpressed *KIF20A* resulted in M2 polarization of TAMs, which might contribute to the promotional effects of *KIF20A* on ovarian cancer progression.

Conclusion

The findings of our study revealed that *KIF20A* depletion and irradiation both impede the development of ovarian cancer. Additionally, *KIF20A* knockdown dramatically increases the radiosensitivity and further suppresses the development of ovarian cancer by regulating *PTEN* expression. Moreover, our data indicated that *KIF20A* could induce M2 polarization of TAMs. These findings suggested that *KIF20A* could accelerate ovarian cancer progression by regulating *PTEN* expression and inducing M2 polarization, providing novel possibilities for ovarian cancer treatment development.

Availability of Data and Materials

The data used to support the findings of this study are available from the corresponding author upon request.

Author Contributions

XQW, XLQ, and ZJL designed the research study. DWZ and RZX performed the research. XLQ and ZJL provided help and advice on experiments. XQW analyzed the data. All authors were involved in the drafting and critical revision of the manuscript. All authors read and approved the final manuscript. All authors have participated sufficiently in the work and agreed to be accountable for all aspects of the work.

Ethics Approval and Consent to Participate

All patients signed the written informed contents, and the project was conducted based on the Declaration of Helsinki statement. This study protocol was approved by the Medical Ethics Committee of Gansu University of Chinese Medicine (2021-48KYSL).

Acknowledgment

Not applicable.

Funding

This research received no external funding.

Conflict of Interest

The authors declare no conflict of interest.

References

[1] Siegel RL, Miller KD, Fuchs HE, Jemal A. Cancer statistics, 2022. CA: A Cancer Journal for Clinicians. 2022; 72: 7–33.

[2] Levy K, Natarajan S, Wang J, Chow S, Eggold JT, Loo PE, *et al*. Abdominal FLASH irradiation reduces radiation-induced gastrointestinal toxicity for the treatment of ovarian cancer in mice. Scientific Reports. 2020; 10: 21600.

[3] Rai B, Bansal A, Patel FD, Sharma SC. Radiotherapy for ovarian cancers - redefining the role. Asian Pacific Journal of Cancer Prevention. 2014; 15: 4759–4763.

[4] Yang L, Zhang B, Xing G, Du J, Yang B, Yuan Q, *et al*. Neoadjuvant chemotherapy versus primary debulking surgery in advanced epithelial ovarian cancer: A meta-analysis of perioperative outcome. PLoS ONE. 2017; 12: e0186725.

[5] Walsh C. Targeted therapy for ovarian cancer: the rapidly evolving landscape of PARP inhibitor use. Minerva Ginecologica. 2018; 70: 150–170.

[6] López-Soto A, Gonzalez S, Smyth MJ, Galluzzi L. Control of Metastasis by NK Cells. Cancer Cell. 2017; 32: 135–154.

[7] Quail DF, Joyce JA. Microenvironmental regulation of tumor progression and metastasis. Nature Medicine. 2013; 19: 1423–1437.

[8] Wu T, Dai Y. Tumor microenvironment and therapeutic response. Cancer Letters. 2017; 387: 61–68.

[9] Hinshaw DC, Shevde LA. The Tumor Microenvironment Innately Modulates Cancer Progression. Cancer Research. 2019; 79: 4557–4566.

[10] Maman S, Witz IP. A history of exploring cancer in context. Nature Reviews. Cancer. 2018; 18: 359–376.

[11] Wang J, Li D, Cang H, Guo B. Crosstalk between cancer and immune cells: Role of tumor-associated macrophages in the tumor microenvironment. Cancer Medicine. 2019; 8: 4709–4721.

[12] Li C, Xu X, Wei S, Jiang P, Xue L, Wang J, *et al*. Tumor-associated macrophages: potential therapeutic strategies and future prospects in cancer. Journal for Immunotherapy of Cancer. 2021; 9: e001341.

[13] Mantovani A, Marchesi F, Malesci A, Laghi L, Allavena P. Tumour-associated macrophages as treatment targets in oncology. Nature Reviews. Clinical Oncology. 2017; 14: 399–416.

[14] Ngambenjawong C, Gustafson HH, Pun SH. Progress in tumor-associated macrophage (TAM)-targeted therapeutics. Advanced Drug Delivery Reviews. 2017; 114: 206–221.

[15] Chen X, Liu Y, Gao Y, Shou S, Chai Y. The roles of macrophage polarization in the host immune response to sepsis. International Immunopharmacology. 2021; 96: 107791.

[16] Weinhäuser I, Pereira-Martins DA, Almeida LY, Hilberink JR, Silveira DRA, Quek L, *et al*. M2 macrophages drive leukemic transformation by imposing resistance to phagocytosis and improving mitochondrial metabolism. Science Advances. 2023; 9: eadf8522.

[17] He Y, Gao Y, Zhang Q, Zhou G, Cao F, Yao S. IL-4 Switches Microglia/macrophage M1/M2 Polarization and Alleviates Neurological Damage by Modulating the JAK1/STAT6 Pathway Following ICH. Neuroscience. 2020; 437: 161–171.

[18] Liang B, Zhou Y, Jiao J, Xu L, Yan Y, Wu Q, *et al*. Integrated Analysis of Transcriptome Data Revealed AURKA and KIF20A as Critical Genes in Medulloblastoma Progression. Frontiers in Oncology. 2022; 12: 875521.

[19] Wu WD, Yu KW, Zhong N, Xiao Y, She ZY. Roles and mechanisms of Kinesin-6 KIF20A in spindle organization during cell division. European Journal of Cell Biology. 2019; 98: 74–80.

[20] Ren X, Chen X, Ji Y, Li L, Li Y, Qin C, *et al*. Upregulation of KIF20A promotes tumor proliferation and invasion in renal clear cell carcinoma and is associated with adverse clinical outcome. Aging. 2020; 12: 25878–25894.

[21] Meng X, Li W, Yuan H, Dong W, Xiao W, Zhang X. KDELR2-KIF20A axis facilitates bladder cancer growth and metastasis by enhancing Golgi-mediated secretion. Biological Procedures Online. 2022; 24: 12.

[22] Zhao X, Zhou LL, Li X, Ni J, Chen P, Ma R, *et al*. Overexpression of KIF20A confers malignant phenotype of lung adenocarcinoma by promoting cell proliferation and inhibiting apoptosis. Cancer Medicine. 2018; 7: 4678–4689.

[23] Jin Z, Tao S, Zhang C, Xu D, Zhu Z. KIF20A promotes the development of fibrosarcoma via PI3K-Akt signaling pathway. Experimental Cell Research. 2022; 420: 113322.

[24] Wu M, Wu X, Han J. KIF20A Promotes CRC Progression and the Warburg Effect through the C-Myc/HIF-1α Axis. Protein & Peptide Letters. 2023; 31: 107–115.

[25] Gao C, Zhang Y, Tian Y, Han C, Wang L, Ding B, *et al*. Circ_0055625 knockdown inhibits tumorigenesis and improves radiosensitivity by regulating miR-338-3p/MSI1 axis in colon cancer. World Journal of Surgical Oncology. 2021; 19: 131.

[26] Huang YJ, Yang CK, Wei PL, Huynh TT, Whang-Peng J, Meng TC, *et al*. Ovatodiolide suppresses colon tumorigenesis and prevents polarization of M2 tumor-associated macrophages through YAP oncogenic pathways. Journal of Hematology & Oncology. 2017; 10: 60.

[27] Yu H, Xu Z, Guo M, Wang W, Zhang W, Liang S, *et al*. FOXM1 modulates docetaxel resistance in prostate cancer by regulating KIF20A. Cancer Cell International. 2020; 20: 545.

[28] Liu B, Su J, Fan B, Ni X, Jin T. High expression of KIF20A in bladder cancer as a potential prognostic target for poor survival of renal cell carcinoma. Medicine. 2023; 102: e32667.

[29] Kawai Y, Shibata K, Sakata J, Suzuki S, Utsumi F, Niimi K, *et al*. KIF20A expression as a prognostic indicator and its possible involvement in the proliferation of ovarian clear cell carcinoma cells. Oncology Reports. 2018; 40: 195–205.

[30] Xiong M, Zhuang K, Luo Y, Lai Q, Luo X, Fang Y, *et al*. KIF20A promotes cellular malignant behavior and enhances resistance to chemotherapy in colorectal cancer through regulation of the JAK/STAT3 signaling pathway. Aging. 2019; 11: 11905–11921.

[31] Song Z, Huang Y, Zhao Y, Ruan H, Yang H, Cao Q, *et al*. The Identification of Potential Biomarkers and Biological Pathways in Prostate Cancer. Journal of Cancer. 2019; 10: 1398–1408.

[32] Shen T, Yang L, Zhang Z, Yu J, Dai L, Gao M, *et al*. KIF20A Affects the Prognosis of Bladder Cancer by Promoting the Proliferation and Metastasis of Bladder Cancer Cells. Disease Markers. 2019; 2019: 4863182.

[33] Lee YR, Chen M, Pandolfi PP. The functions and regulation of the PTEN tumour suppressor: new modes and prospects. Nature Reviews. Molecular Cell Biology. 2018; 19: 547–562.

[34] Jiang TY, Cui XW, Zeng TM, Pan YF, Lin YK, Feng XF, *et al*. PTEN deficiency facilitates gemcitabine efficacy in cancer by modulating the phosphorylation of PP2Ac and DCK. Science Translational Medicine. 2023; 15: eadd7464.

[35] Wang L, Wang C, Sarwar MS, Chou P, Wang Y, Su X, *et al*. PTEN-knockout regulates metabolic rewiring and epigenetic reprogramming in prostate cancer and chemoprevention by triterpenoid ursolic acid. FASEB Journal. 2022; 36: e22626.

[36] Yan Y, Huang H. Interplay Among PI3K/AKT, PTEN/FOXO and AR Signaling in Prostate Cancer. Advances in Experimental Medicine and Biology. 2019; 1210: 319–331.

[37] Wang Z, Zhou H, Cheng F, Zhang Z, Long S. miR-21 Negatively Regulates the PTEN-PI3K-Akt-mTOR Signaling Pathway in Crohn's Disease by Altering Immune Tolerance and Epithelial-Mesenchymal Transition. Discovery Medicine. 2022; 34: 45–58.

[38] Tang Z, Zhao P, Zhang W, Zhang Q, Zhao M, Tan H. SALL4 activates PI3K/AKT signaling pathway through targeting PTEN, thus facilitating migration, invasion and proliferation of hepatocellular carcinoma cells. Aging. 2022; 14: 10081–10092.

[39] Bassi C, Fortin J, Snow BE, Wakeham A, Ho J, Haight J, *et al*. The PTEN and ATM axis controls the G1/S cell cycle checkpoint and tumorigenesis in HER2-positive breast cancer. Cell Death and Differentiation. 2021; 28: 3036–3051.

[40] Zhao W, Han T, Li B, Ma Q, Yang P, Li H. miR-552 promotes ovarian cancer progression by regulating PTEN pathway. Journal of Ovarian Research. 2019; 12: 121.

[41] Zhang S, Li D, Zhao M, Yang F, Sang C, Yan C, *et al*. Exosomal miR-183-5p Shuttled by M2 Polarized Tumor-Associated Macrophage Promotes the Development of Colon Cancer via Targeting THEM4 Mediated PI3K/AKT and NF-κB Pathways. Frontiers in Oncology. 2021; 11: 672684.

[42] Baig MS, Roy A, Rajpoot S, Liu D, Savai R, Banerjee S, *et al*. Tumor-derived exosomes in the regulation of macrophage polarization. Inflammation Research. 2020; 69: 435–451.

[43] Su S, Liu Q, Chen J, Chen J, Chen F, He C, *et al*. A positive feedback loop between mesenchymal-like cancer cells and macrophages is essential to breast cancer metastasis. Cancer Cell. 2014; 25: 605–620.

[44] Noy R, Pollard JW. Tumor-associated macrophages: from mechanisms to therapy. Immunity. 2014; 41: 49–61.

[45] Liu Q, Yang C, Wang S, Shi D, Wei C, Song J, *et al*. Wnt5a-induced M2 polarization of tumor-associated macrophages via IL-10 promotes colorectal cancer progression. Cell Communication and Signaling. 2020; 18: 51.